Geodinamica Acta

Geodinamica Acta 18/6 (2005) 401–416

Neogene to Quaternary stress field evolution in Lesser Caucasus and adjacent regions using fault kinematics analysis and volcanic cluster data

Ara Avagyan [a], Marc Sosson [b, *], Herve Philip [c], Arkadi Karakhanian [d], Yann Rolland [b], Rafael Melkonyan [a], Samira Rebaï [e], Vahan Davtyan [d]

[a] *Institute of Geological Sciences, National Academy of Sciences of Armenia, 24a Baghramian avenue, Yerevan, 375019, Armenia.*
[b] *Géosciences Azur, CNRS-University of Nice-Sophia Antipolis, UMR 6526, 250 rue A. Einstein, 06560 Valbonne, France.*
[c] *Laboratory of Geophysics, Tectonics and Sedimentology, UMR 5573, Montpellier-2 University, France.*
[d] *GEORISK Scientific Research Company, 24a Baghramian avenue, Yerevan, 375019, Armenia.*
[e] *SIEE, Parc 2000, Av Y. Montand, 34000 Montpellier, France.*

Received: 15/04/2005, accepted: 04/11/2005

Abstract

In the Great Caucasus, the Lesser Caucasus and Eastern Turkey, the distribution of Neogene to Quaternary volcanic cluster geometries, paleo-stress field data of the Lesser Caucasus area (Republic of Armenia) and the P axes of earthquakes focal mechanisms show the scale and time variability of the stress field since the beginning of the Arabia-Eurasian collision. In addition to the general N-S compression orientation, two other NW-SE and NE-SW secondary orientations are observed. Both orientations were successively significant for some period of tectonic activity. The first one was dominant between the Paleogene and the end of the Lower Miocene and the second one has prevailed between the Upper Miocene and the Quaternary. On a regional scale the principal stress axes orientations are mainly controlled by the Arabian-Eurasian plate convergence and have changed with time. Local stress orientations have been significantly influenced by secondary blocks motions and their geometries.

Résumé

De nouvelles études sur la distribution des alignements volcaniques néogènes et quaternaires, les paléo-champs de contraintes du Petit Caucase et les mécanismes au foyer des séismes dans le Caucase et la Turquie orientale permettent de caractériser des variations spatiale et temporelle de l'orientation du champ de contrainte depuis la collision Arabie-Eurasie.

Les résultats montrent que la principale orientation de l'axe de compression est N-S et qu'il existe deux autres directions secondaires NW-SE et NE-SW. Ces deux dernières sont liées à des périodes d'activité tectoniques successives. La première NW-SE a dominé la période comprise entre le Paléogène et le Miocène inférieur. La seconde NE-SW caractérise la période Miocène supérieur à Quaternaire.

À l'échelle régionale l'axe principal de compression est clairement lié à la convergence Arabie-Eurasie et a varié de direction depuis la collision. Localement les champs de contraintes sont liés à des mouvements de blocs et à leur géométrie.

Keywords: Collision; Stress field; Volcanic clusters; Lesser Caucasus; Armenia

Mots clé : Collision ; Champ de contrainte ; Alignements volcaniques ; Petit Caucase ; Arménie

* Corresponding author.
Tel.: +33 (0)492942655 - Fax: +33 (0)492942610
E-mail address: sosson@geoazur.unice.fr

1. Introduction

Since Upper Jurassic times, the Great Caucasus, Trans-Caucasus and Eastern Turkey alpine (s.l.) tectonic evolution has been controlled by subduction of the Neotethys ocean, associated obductions of the Neotethys and collisions of continental blocks [1, 2, 3 and 4]. A result of the last collision is the indentation of the Eurasian plate by Arabia. Due to oceanic lithosphere remnants in the Black and Caspian seas, the collisional deformations are concentrated within the continental lithosphere of the Caucasus and surrounding areas (Fig. 1). Consequently, distributed active structures underlain by subducted lithosphere affect a wide domain from the peri-Arabic frontal thrusts to the Northern Great Caucasus (Fig. 2).

The recent stress field has produced a wide range of active faults in the region under consideration (Fig. 2) [e.g. 5, 6, 7 and 8] in response to N-S to NNE-SSW trending Arabian and Eurasian plates convergence [5, 6, 9, 10, 11, 12 and 13]. Four simultaneously existing types of neotectonic faults are present comprising: (1) NE striking sinistral strike-slip faults; (2) NW striking dextral strike-slip faults; (3) E striking thrusts; (4) and N trending normal faults (Fig. 2). The major active faults form large top to the North structural arcs.

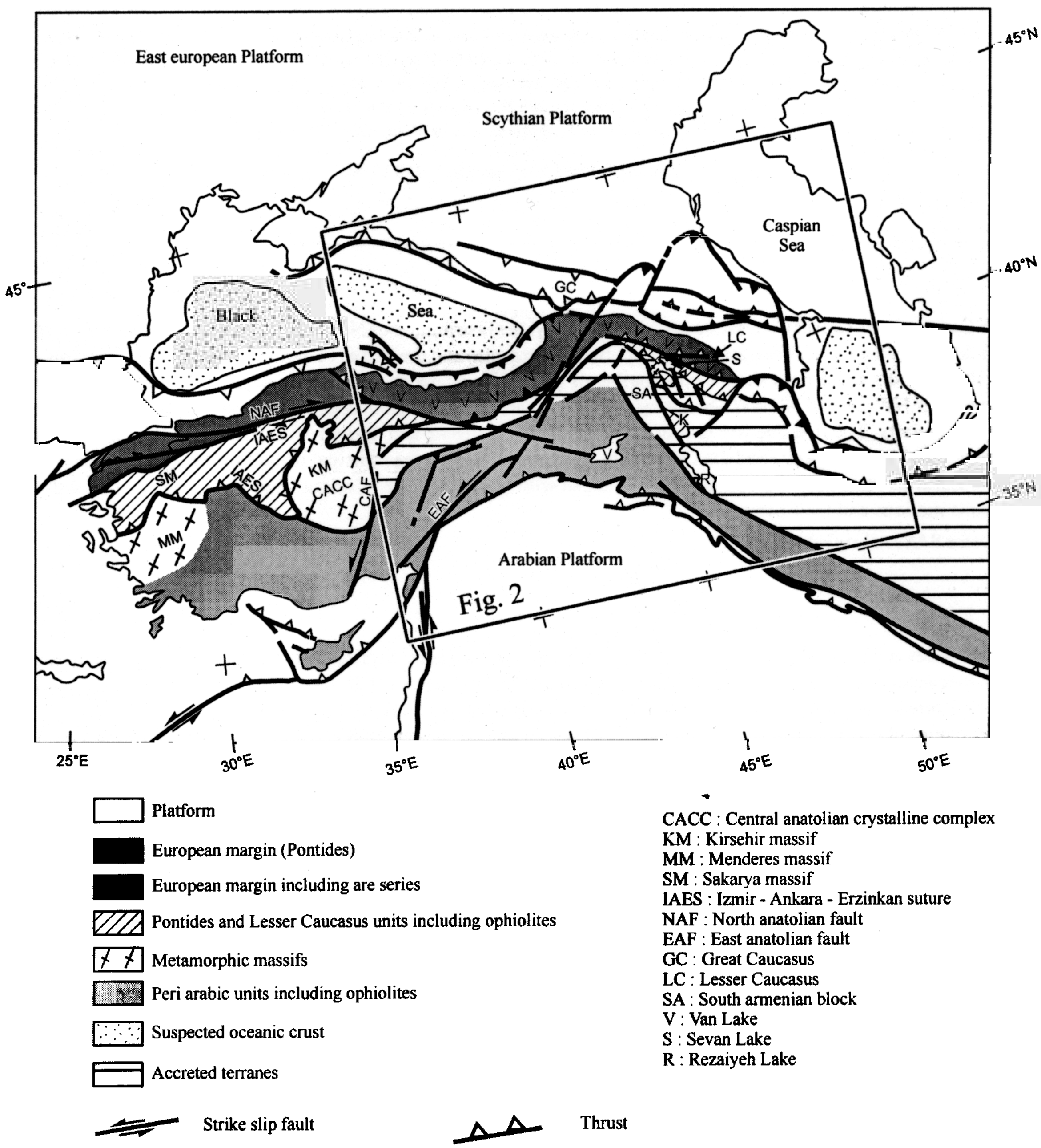

Fig. 1 Structural map of the Arabia-Eurasia collision area.
Carte structurale de la zone de collision Arabie-Eurasie.

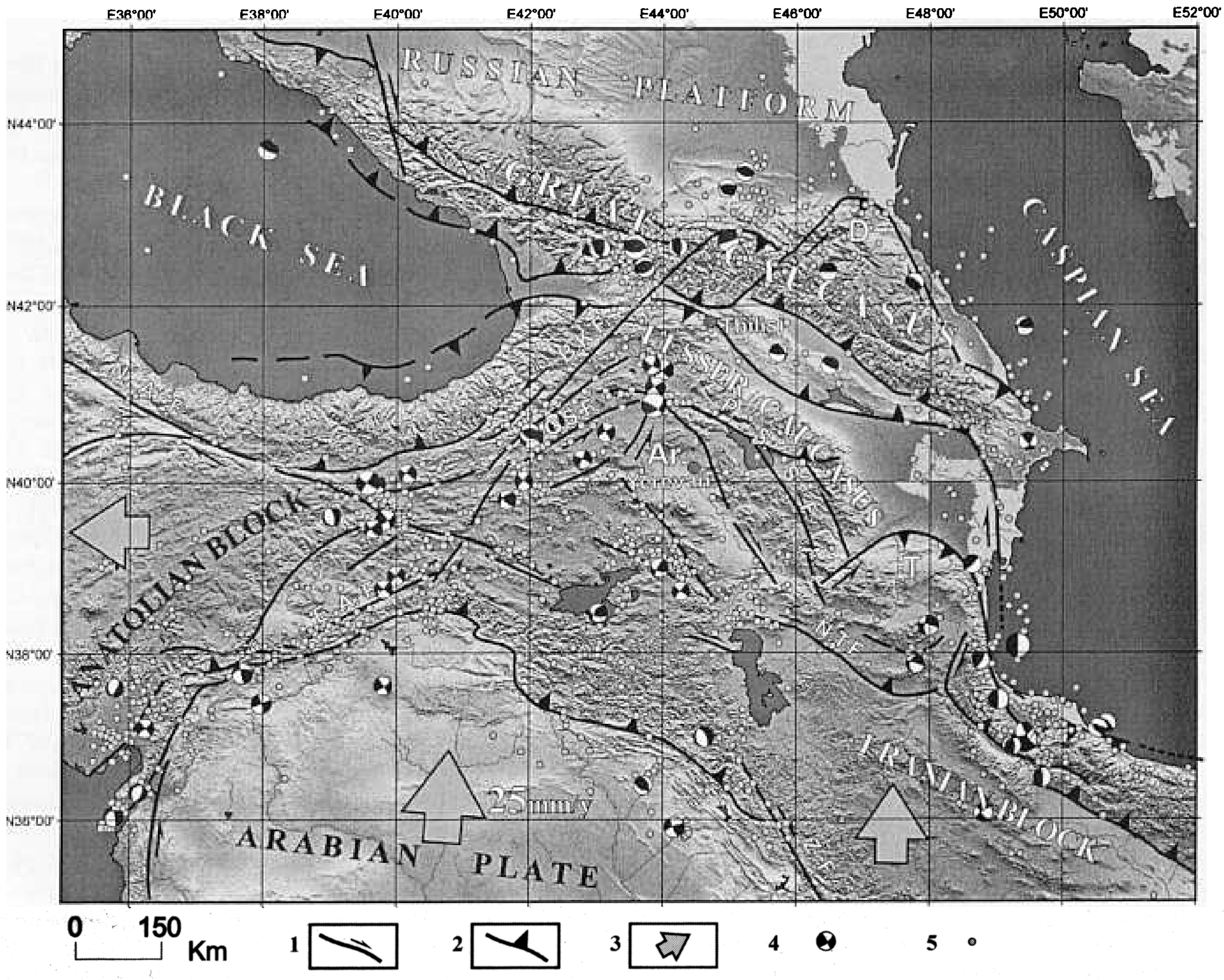

Fig. 2 Active tectonics north of the Arabian plate (modified from Philip *et al.*, 1989, 2001; Rebaï *et al.*, 1993) location on figure 1. (1) Major strike-slip faults; (2) major thrust faults; (3) relative motion of blocks with respect to Eurasia; 4. focal mechanisms of Mw >4.8 earthquake (CMT Harvard); (5) instrumental seismicity of 3 < Mb < 4.9 (USGS-NEIC). Ar—Armenia; D—Dagestan; T—Talish; E.A.F.—East Anatolian fault; N.A.F.—North Anatolian fault; P.S.S.F.—Pambak–Sevan–Sunik fault; Z.F.—Zagros fault; N.T.F.—North Tebriz fault; G.S.F—Geltarechka-Sarikhamish fault.

Carte de la tectonique active du nord de la plaque Arabe (modifiée de Philip *et al.*, 1989, 2001 ; Rebaï *et al.*, 1993), (1) principaux décrochements ; (2) principaux chevauchements ; (3) mouvement relatif des blocs par rapport à l'Eurasie ; 4. Mécanismes aux foyer des séismes de magnitude Mw > 4.8 (CMT Harvard) ; (5) Séismicité 3 < Mb < 4.9 (USGS-NEIC). Ar : Arménie ; D : Dagestan ; T : Talish ; E.A.F. : Faille Est Anatolienne ; N.A.F. : Faille nord Anatolienne ; P.S.S.F. : Faille Pambak—Sevan–Sunik ; Z.F. : Faille du Zagros ; N.T.F. : Faille Nord Tebriz ; G.S.F : Faille Geltarechka-Sarikhamish.

All these crustal structures are related to the collisional evolution of the region and in particular some of them correspond to the limits of accreted terranes emplaced since the Upper Cretaceous. Nevertheless in the Lesser Caucasus, the chronology of deformations and the stress field evolution is not well constrained during Neogene to Quaternary times.

The aim of this paper is to study the evolution of the stress field in the Lesser Caucasus and adjacent regions from the Neogene to the Quaternary in order to determine the chronology of stress regime changes and highlight the role of that inherited structures play in localising recent deformation. The study region is enclosed between main rigid blocks (Arabia, Eurasia), and escaping secondary blocks (Iran and Anatolia). This region (Armenian highland) due to its central tectonic position in the central part of a continental collision is submitted to intense shortening.

A detailed stress field study based on active structures kinematics, GPS measurements, focal mechanisms, fault kinematics and volcanic cluster data are evaluated to characterize the change of the stress field in space and time. The data allow us to examine the influence of inherited structures and the rheologic behaviour of the crust.

2. Kinematic and Geodynamic setting

The Africa-Eurasia convergence started during the Upper Cretaceous [e.g. 14, 15, 16, 17 and 18] (Fig. 3). Since Early Upper Cretaceous times the convergence velocity has varied from 0.9 to 3 cm. a^{-} [15]. The Upper Cretaceous—Lower Tertiary period was characterized by subduction of Neotethys ocean beneath the Eurasian active margin, and by the accretion of the various continental blocks originating at the Gondwana [e.g. 18 and 19].

Continental rifting in the Red Sea region was initiated at the Oligocene–Miocene boundary (23 Ma) [20] and was followed by separation of the Arabian from the African plate and by collision of Arabia with the Iranian margin along the Zagros belt. Northward drift of the Arabian plate was accommodated by initiation of several crustal strike-slip faults such as the Dead Sea Fault zone and the North and East Anatolian faults [9, 10, 18, 21, 22, 23, 24 and 25].

The onset of left-lateral motion along the Dead Sea Fault zone [26] occurred in the mid-Miocene (10-13 Ma). Since its initiation, the convergence velocity rate of Arabia relative to Eurasia has increased to 2.5-2.6 cm. a^{-1} [15, 18 and 27] and the ongoing Arabian northward drift has resulted in tectonic escape of the Anatolian and Iranian blocks, towards the West and North-East, respectively.

During the Miocene an intense shortening phase occurred due to the Arabian-Eurasian convergence, which has led to crustal thickening and uplift [e.g. 25] and produced the high elevated Armenian plateau (Armenian highland, about 1800 meters on average).

Because the relative movement velocity and the convergence direction have been variable, it is important in the stress field analysis to know the evolution of relative motion between plates (Arabia and Eurasia) controlling the regional tectonics.

Three main changes in plate motion are known.

(i) The Arabian plate moved to the NW along the Eurasian margin with the onset of the Arabian-Eurasian collision during the Lower Oligocene (35 Ma) [17].

(ii) Zonenshain *et al.* [15] demonstrate a change from N-S to NW-SE convergence during the Lower Miocene.

(iii) In the Middle Miocene the movement of the Arabian plate again became top to the north and in eastern part, top to the NNE [15]. Since the Middle Miocene the stress field probably remained relatively constant [e.g. 7].

The Arabian-Eurasian convergence (estimated at 20-30 mm. a^{-1} [28]) resulted continental collision and tectonic escape of the Anatolian and Iranian blocks. The central region in front of the Arabian plate experienced a phase of intense shortening [5, 6, 9, 10 and 11]). The prevalent carbonate and volcanic series were folded during the Neogene collision (Fig. 4) [7, 18 and 29]. In eastern Anatolia, western Iran, Armenia and the Caucasus, numerous active strike-slip and reverse faults form large structural wedges bounded by dextral strike-slip faults on the eastern flank and sinistral strike-slip faults on the western flank and with tips oriented to the north and northeast (Fig. 2). The strain field is characterized by structures such as east-west folds and thrust faults, oblique strike-slip, and north trending normal faults [7, 13 and 18]. These active tectonics features are produced in general by N-S compression and E-W extension, characteristic to strike-slip stress regime.

As a result of terrane accretion and Arabian plate collision, the tectonic evolution of the Lesser Caucasus is mainly controlled by lithospheric anisotropies such as ophiolitic sutures and faults delimiting continental blocks. The stress field can be locally disturbed by these mechanical anisotropies.

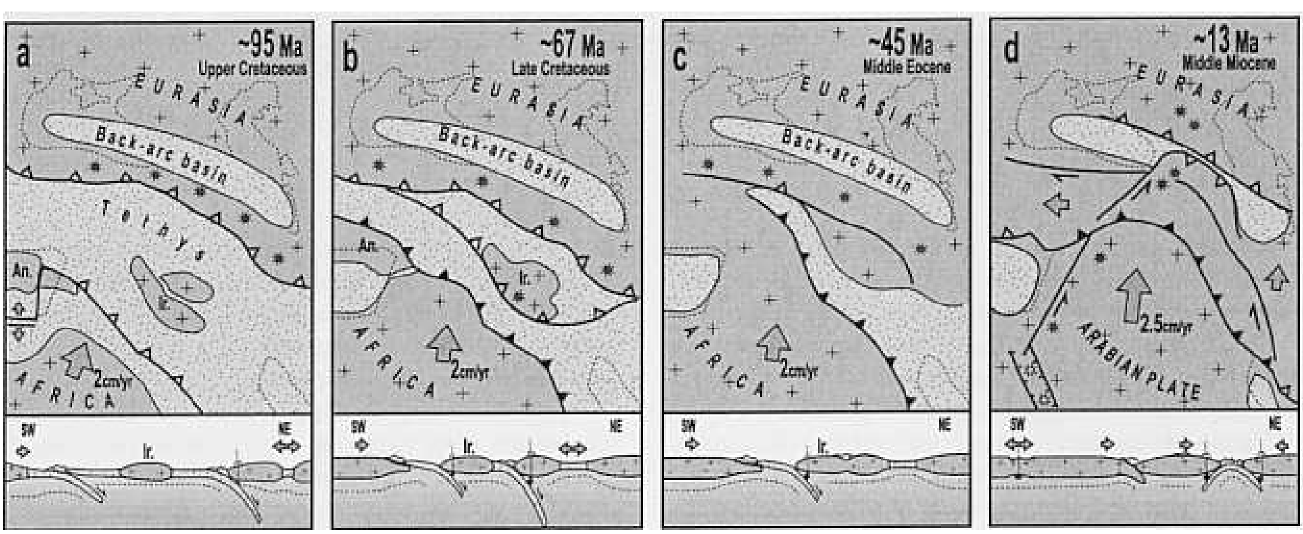

Fig. 3 Geodynamic evolution of the Caucasus region modified from Philip *et al.*, (1989), Ir.: Iranian block, An.: Anatolian block.

Évolution géodynamique du Caucase modifiée de Philip *et al.*, (1989), Ir. : Bloc Iranien, An. : Bloc Anatolien.

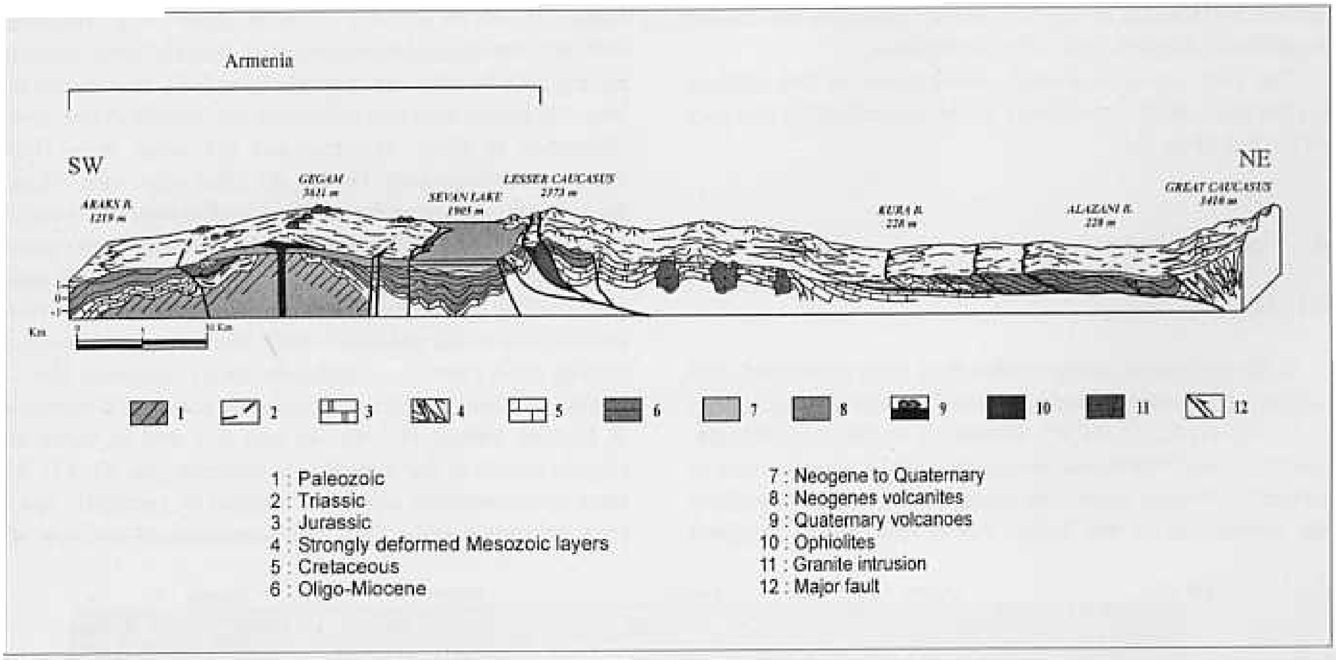

Fig. 4 Block diagram showing a NE-SW Lesser Caucasus cross section from the southern slope of the Great Caucasus to the Gegam volcanic axis modified from Milanovski (1968).

Bloc diagramme d'une coupe NE-SW du Petit Caucase à partir du flanc sud du Grand Caucase jusqu'à l'axe volcanique de Gegam (Arménie) modifiée de Milanovski (1968).

3. Recent stress and strain field data

In addition to data from active tectonics (Fig. 2) we have analyzed recent kinematic data obtained by GPS [24, 30 and 31] and focal mechanisms obtained instrumentally from earthquakes [32 and 33]. The calculated P axis orientation and movement relative to Eurasia by GPS measurements are shown in figure 5. The P axis data provide evidences for three dominant compression orientations in the studied area: N-S, N-NW and NNE (Fig. 5). Testifying for a spatial change in the stress regime these orientations are observed practically all over the studied area. Since the static stress field develops in the upper crust down to the brittle-ductile transition, the observed variability in P axis orientation can be interpreted as micro-block movement in response to the stress from variable distance. It is important to note the influence of active faults on the P axis orientation. One part of the active faults, formed at the beginning of the continental collision, are the result of the initial stress field and local geological anisotropies.

Further, as shown by the GPS strain data (Fig. 5), the movement of micro-blocks, limited by the main active faults, is not uniform. In the southern part the dominant motion is towards the N-NW, while in the northern area mainly NNE motions are observed. According to GPS measurement the relative movement of the central part of the studied area (between latitudes of 40.00N- 42.00N and longitudes of 44.00E-46.00E in figure 2 and 5) displays a N-NE orientation with respect to Eurasia. In contrast, the NUVEL 1A data predict a NNW orientation (table 1). This result is obtained using the UNAVCO Facility (Colorado, USA) plate motion calculator that allows us to use different models (GSRM v1.2; REVEL 2000; APKIM2000.0; ITRF2000; NUVEL 1A; NUVEL 1) to derive motion rates and directions for various locations [27, 28, 34, 35, 36, 37 and 38]. These last results are in agreement with the data of Yunga [39] who studied the seismotectonic deformation of the Caucasus region based on the slips defined by in earthquake sources. Yunga [39] predicted a NNW main compression orientation for the area

Table 1
Calculated relative movement according to NUVEL 1A model.
Mouvement relatif calculé d'après le modèle NUVEL 1A.

Model	Latitude	Longitude	Speed mm/yr	Azimuth (cw from N)	N Vel. mm/yr	E Vel. mm/yr	Plate (reference)
NUVEL 1A	40° 17' 16" N 40.287778°	44° 24' 16" E 44.404444°	27.62	338.16°	25.64	−10.27	Arabia (Eurasia)
NUVEL 1A	41° 2' 33" N 41.042500°	44° 48' 45" E 44.812500°	28.09	337.43°	25.94	−10.78	Arabia (Eurasia)

limited by latitudes of 40.00N-38.00N (southern part of the Republic of Armenia and adjacent regions).

The two opposite motion orientations in the studied region indicate the complexity of the strain field in that part of the belt (Fig. 5).

4. Volcanic cluster

4.1. Volcanic setting

In the study area, many studies have been concerned with volcanism since the Jurassic times and its tectonic origins [e.g. 7, 11, 40, 41, 42, 43, 44, 45, 46 and 47]. In the Lesser Caucasus (Republic of Armenia) magmatic activity from Jurassic to Upper Cretaceous times was mostly arc-type and caused by the subduction of the Tethys ocean and related marginal basins [18, 48, 49 and 50]. Since the onset of the continental collision, volcanism has evolved with bimodal character comprising both basaltic and rhyolitic lavas [45]. In Armenia two stages of intracontinental volcanism are identified: one during Oligocene to Early Miocene and the other from Upper Miocene to Quaternary. During the latter stage vast volcanic massifs and cones were formed in all volcanic provinces of the Armenian highland [45]. Continental collision led to crustal thickening, tectonic uplift and associated extensional structures causing rise in the geothermal gradient and local crustal melting and acidic volcanism [45]. The most recent volcanic activity from Pliocene to Holocene times comprises the volcanism of Nemrout, Sipan, Tondourek and Ararat volcanoes in Eastern Turkey [11, 41, 46 and 51], and in Sunik and Gegam massif in the Republic of Armenia [46, 52, 53]. The most recent volcanic activity is testified by petroglifs curved on a volcanic boulder (Fig. 6) representing an eruption of a

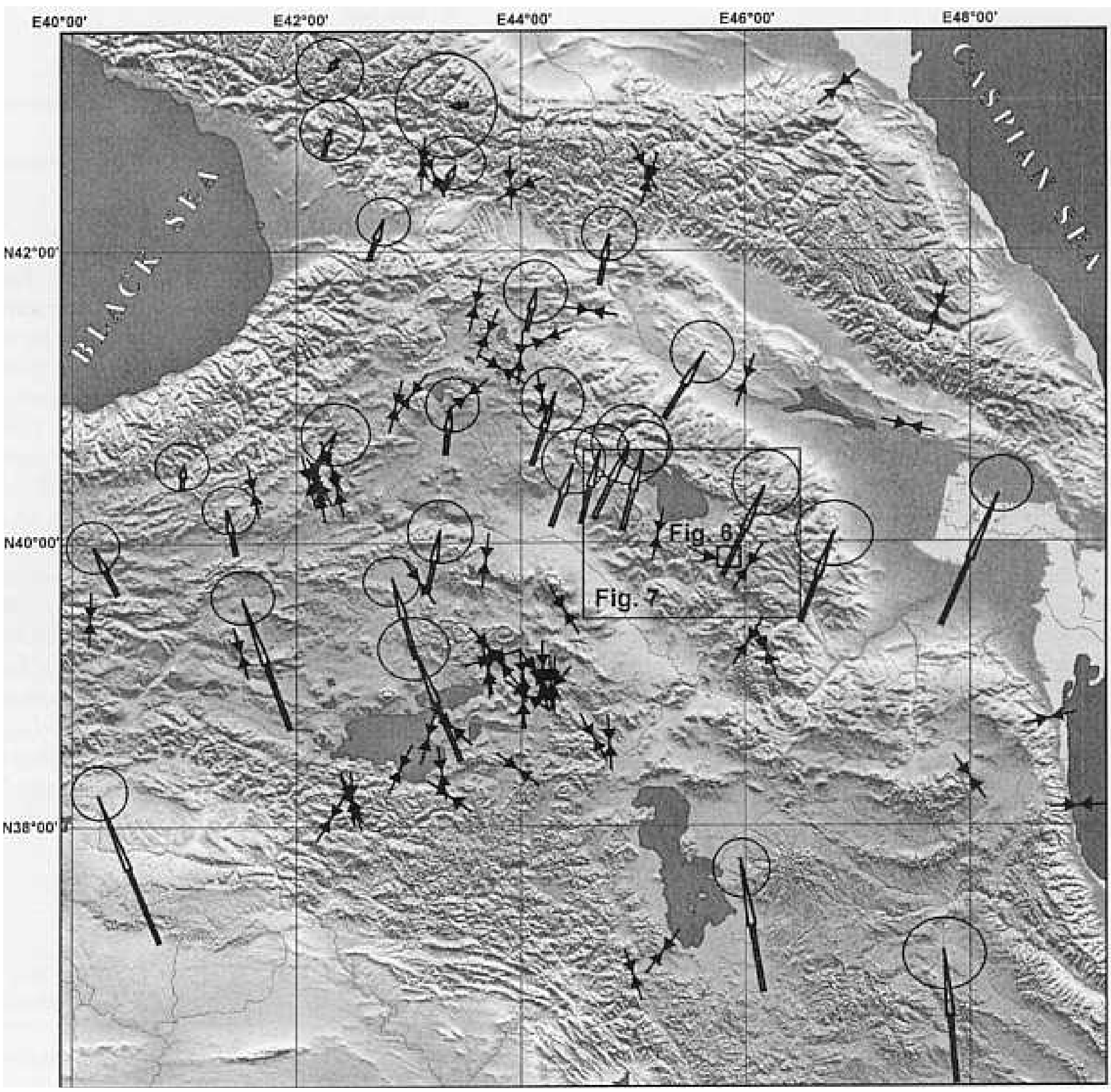

Fig. 5 GPS (Reilinger *et al.*, 1997; McClusky *et al.*, 2000; Vernant, 2003) and P axis data (Tovmassian *et al.*, 1997; Hessami *et al.*, 2003).
Données GPS (Reilinger *et al.*, 1997; McClusky *et al.*, 2000; Vernant, 2003) et axes P (Tovmassian *et al.*, 1997 ; Hessami *et al.*, 2003).

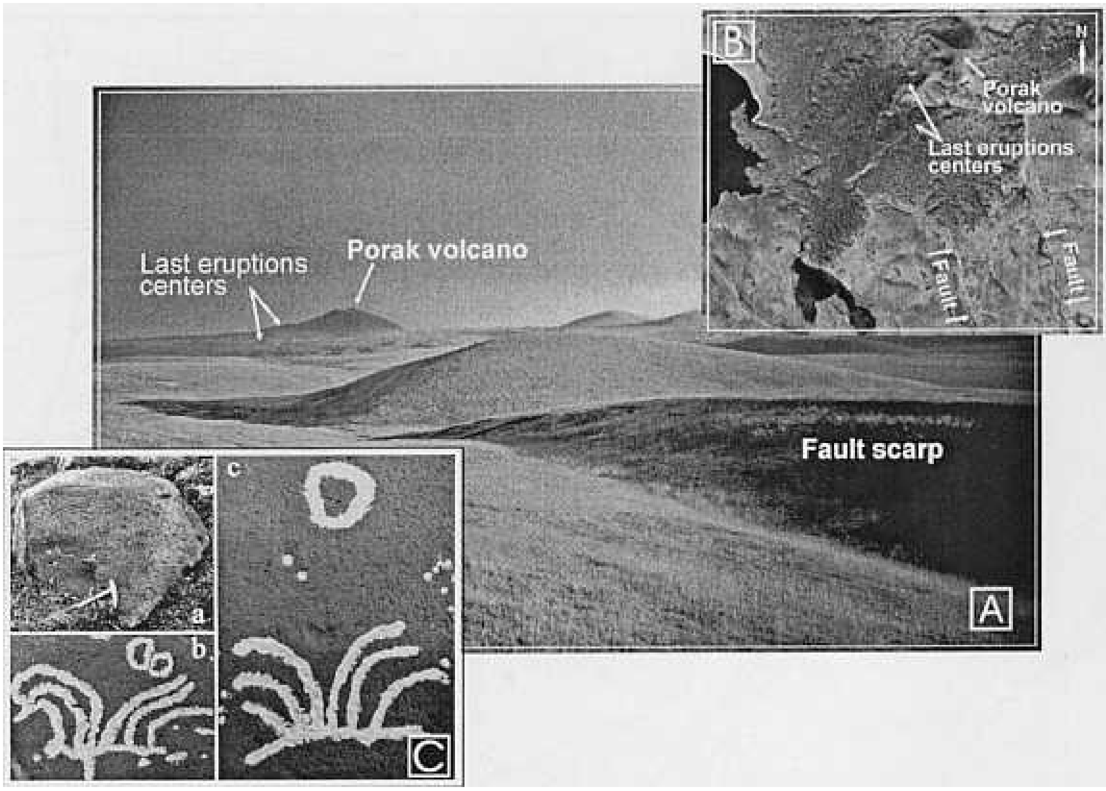

Fig. 6 Petroglifs curved on the basaltic boulder representing a volcanic eruption discovered in 1998 in Sunik area, location on figure5 (Avagyan, 2001; Karakhanian *et al.* 2002; Avagyan *et al.*, 2003). A: the view of the fault scarp (eastern in the B) and Porak volcano; B: satellite image of the Porak volcano area; C: petroglifs found near the site shown in the photo A, a: basaltic boulder with petroglifs, b and c: petroglif fragments with tooth-paste on it.

Pétroglyphes sur un bloc de basalte représentant une éruption volcanique. Découvert en 1998 dans la région de Sunik (Arménie) la localisation est montrée sur la figure 5, (Avagyan, 2001 ; Karakhanian *et al.* 2002 ; Avagyan *et al.*, 2003). A : Escarpement de faille (à l'est de l'image B) et volcan Porak ; B : image satellite de la zone volcanique de Porak ; C : Pétroglyphe trouvé près du site montré sur la photo A, a : bloc de basalte quaternaire avec les pétroglyphes, b et c : Fragments de pétroglyphe blanchit pour l'observation (« avec du dentifrice »).

nearby volcano in the Sunik area (Fig. 7) [46, 52 and 53] on the western fault branch south of the Porak volcano (B in Fig. 6). From the petroglif site the last eruption centres situated on the continuation of the fault trace are clearly visible (A in Fig. 6). The nearest one is not a classic volcanic cone and has produced lava flows on both sites of the fault.

4.2. New data and interpretations

In our study we have used volcanic alignments of the same age as indicators of the tectonic regime and stress axis orientation. Such an approach has been used by several researchers in Armenian highland [e.g. 42] and in other regions [44, 54, 55, 56, 57, 58 and 59]. In this prospect we have used satellite images (SPOT, Corona, Landsat) covering the Republic of Armenia and adjacent regions to identify linear clusters, ridges and elongated shapes of Neogene Quaternary volcanoes (Fig. 7). The data show the importance of extensional and strike-slip tectonics related to the tensional fractures, pull-apart, tail-crack or horsetail structures [e.g. 44 and 46].

Most volcanoes in the Republic of Armenia and adjacent area form clusters of different length from several kilometres up to 50 km and are clearly rooted on tension fractures (Fig. 7, 8, and 9). The volcanic cones in the whole of the axial part of the Gegam massif form a N-NW trending (N166°E) cluster of slightly more than 50 km in length. In the massif the smaller clusters at a length of 5-10 km strike slightly more to the NW (N146°-N155°E). This provides evidence for fault depth difference on which clusters of various lengths are rooted [44, 49 and 50]. Taking into account a crustal depth in the studied area of about 50 km [e.g. 18], we suggest that the geological structures controlling the big Gegam and Sunik major clusters influence the entire thick of the crust. This is supported by occurrences of basalt volcanism, probably of mantle origin, within the fissured areas [46]. On the other hand, within smaller clusters several km in length magmas with crustal origin are present [44 and 50].

The orientations of volcanic clusters range from NW-SE to NE-SW. To the east of the Gegam axial cluster two small clusters have a N-S trend and one cluster has a NE-SW (N62°) orientation. To the east, all observed clusters and elongated cone groups have NW-SE orientation. Despite the general E-W orientation of the Vardenis massif, which could be inherited from Oligo-Miocene structures, the volcanic clusters have N-S and NW-SE orientations (N137° E-N169°E).

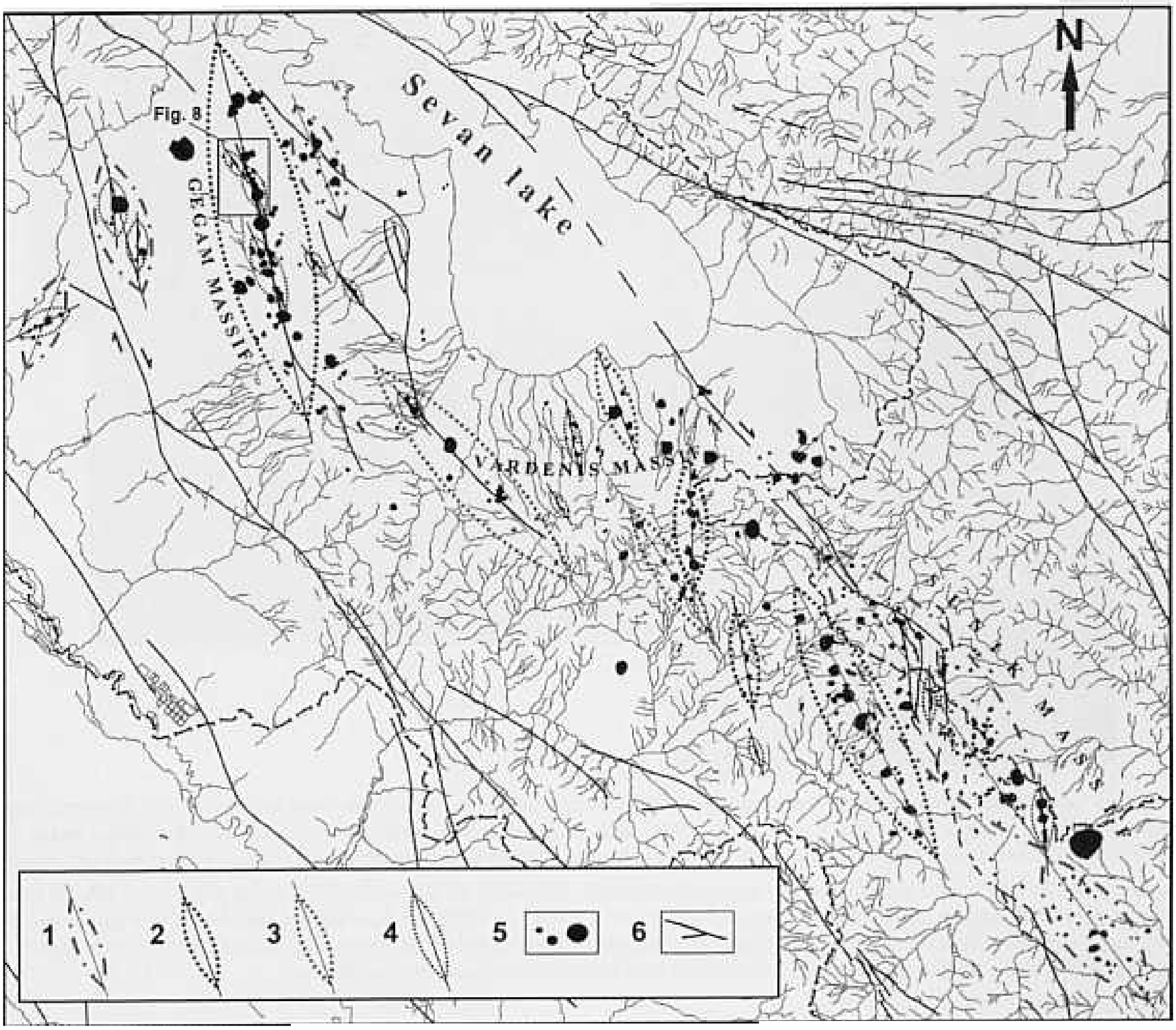

Fig. 7 Neogene to Quaternary volcanic clusters in the SE of the territory of the Republic of Armenia. Location is shown on figure5, 1: Elongated volcanic cones groups, 2: volcanic clusters well recognized, 3: supposed volcanic clusters, 4: small volcanic clusters, 5: volcanic cones, 6: active faults.

Alignements volcaniques Néogène à Quaternaire dans le SE de l'Arménie, localisation de la zone sur la figure5. 1 : Groupes allongés de cônes volcaniques, 2 : alignements volcaniques bien reconnus, 3 : alignements volcaniques supposés, 4 : petits alignements volcaniques, 5 : cônes volcaniques, 6 : Failles actives.

Recent GPS data indicate an extension rate of 2.36 ± 0.9 mm. a^{-1} with the azimuth of N 55° in the Gegam and Vardenis massifs area [60].

As shown in figure 7 the big clusters are oriented principally NW-SE in central and southern parts of the Republic of Armenia and are either emplaced on deeply rooted faults of the same orientation or are parallel to them. In the case of smaller clusters we also have nearly N-S and NE-SW orientations. These general cluster orientations are more consistent (parallel) with the NUVEL 1A model [27, 28, 34, 35, 36, 37, 38 and 39] data and show the same orientation of relative movements of the area with respect to Eurasia as the GPS data obtained from NW of Iran [31].

If we consider data for the area including the Republic of Armenia, Southern Georgia and Eastern Turkey [44] we observe another permanent cluster orientation of NNE-SSW sited principally in the West (Fig. 10). Thus the volcanic cluster in the study area forms a cluster wedge with top (near the Javakhety area) oriented to the North (J in figure 10). It is important to note that the active faults in the same area also form similar structural wedges with left-lateral strike-slip faulting to the West and right-lateral faulting to the East [6]. This means that there is a good spatial correlation between active faults and volcanic activity. It is also important to note that the some clusters are controlled by pull-apart and tail-crack structures [44 and 46]. The GPS data for the area showing the N-NE orientation [24 and 30] of the convergence movement are consistent with the NNE-SSW cluster orientation on the Eastern flank of the volcanic cluster wedge (Fig. 10).

5. Fault kinematics analysis

The previous fault kinematics analyses [18, 61, 62, 63 and 64] and new results (about 30 stations) obtained from the

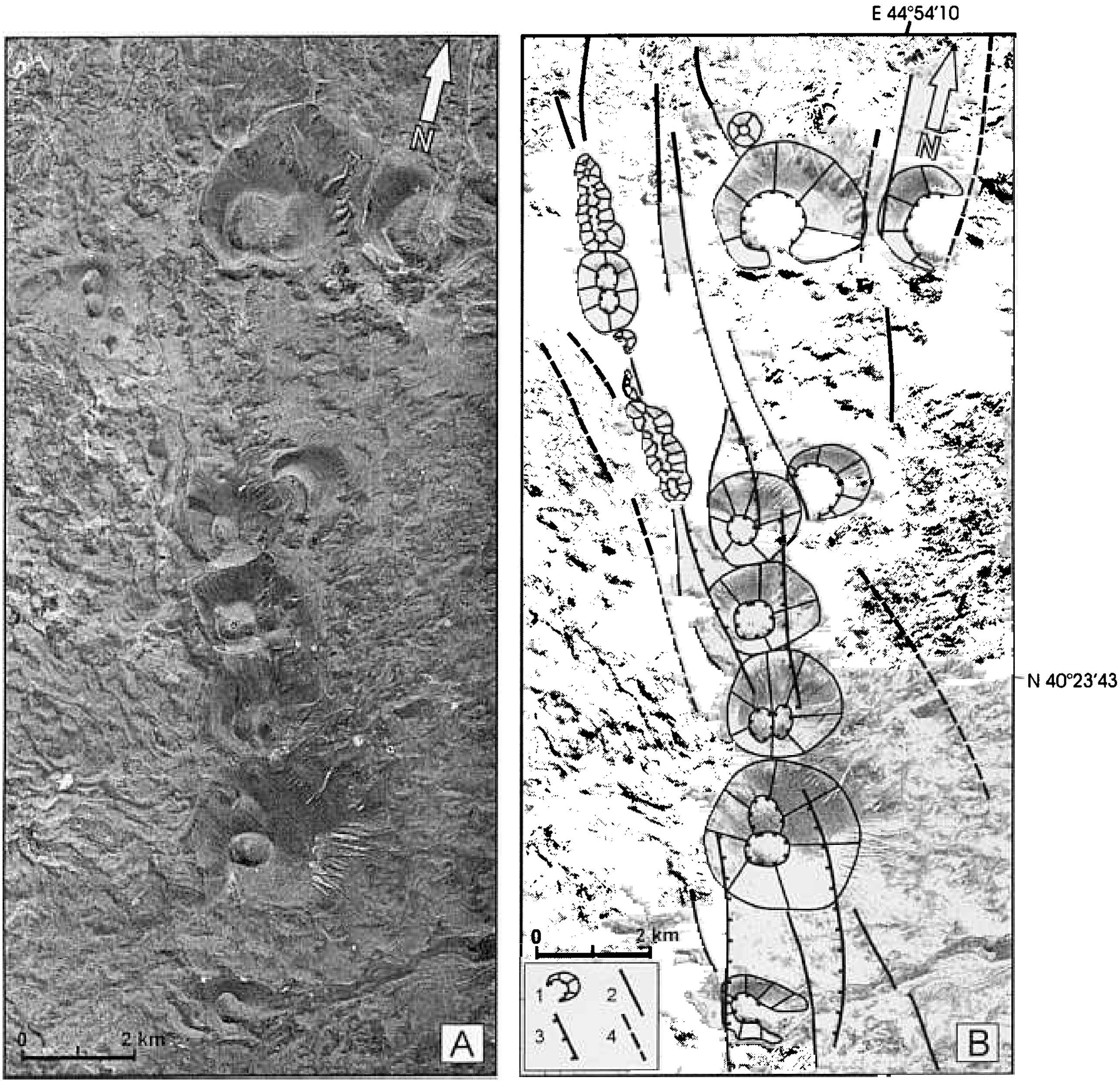

Fig. 8 Fragment of the Gegam axial cluster, location on figure 7. A: on a Corona satellite image, B: interpretation, 1: volcanoes, 2: faults, 3: normal faults, 4: supposed faults.

Fragment de l'alignement volcanique de l'axe de Gegam, localisation sur la figure A : sur une image satellite Corona, B : interprétation, 1 : volcans, 2 : failles supposées.

Lesser Caucasus area microtectonic stations indicate three principal orientations of the compression axis: N-S, NE-SW and NW-SE (Fig. 10). Paleostress axis orientations have been calculated by inversion of slip vectors measured on fault planes using the method proposed by Etchecopar *et al.* [65]. This method provides the possibility to calculate different stress fields corresponding to several groups of fault striation data. Fault kinematics data are obtained from rocks of various ages (from Devonian to Quaternary) to resolve paleo-stress orientations. The paleo-orientation results can be compared with the earthquake P axis data related to the present stress field.

The variability of stress orientation is evident when active faults approached so we collected fault kinematics measurements as far from them as possible. On the other hand, the high density of active faults does not prevent perturbations in stress direction. The stress variability in the same blocks is observed with focal mechanisms (Fig. 5). For paleo-stress data we have also observed such variability (Fig. 11) although here the time interval between stress age indicators could be considerable. We can have also stress field changes. Figure 12 is an example of paleo-stress data collected in the Azat river area. Preliminary analyses of micro fault data allow us to separate fault kinematics data groups

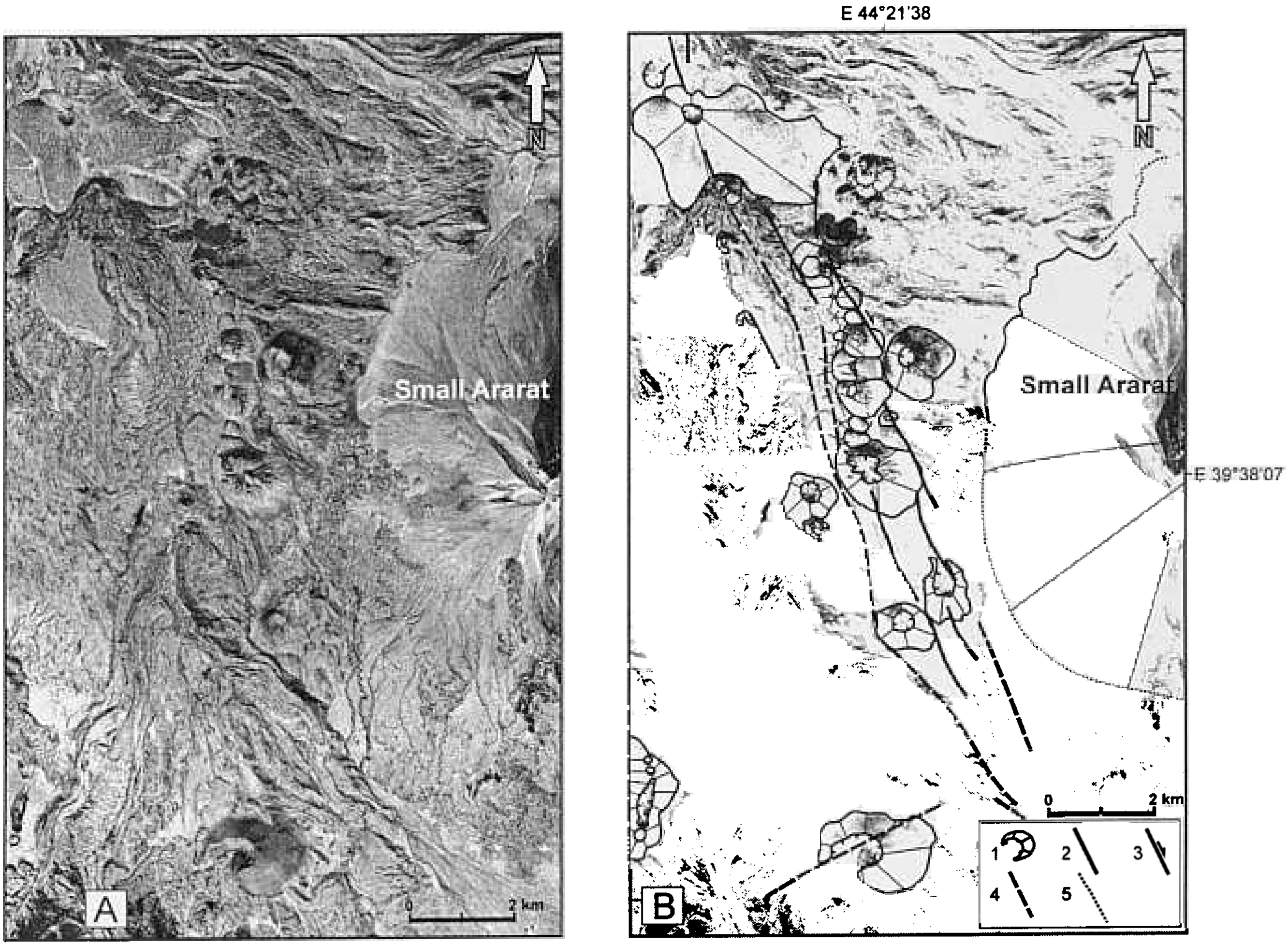

Fig. 9 Ararat cluster between Great and Small Ararat. Location is shown on figure 10. A: on the satellite image, B: interpretation, 1: volcanoes, 2: faults, 3: strike-slip faults, 4: supposed faults, 5: supposed volcano outlines.

Alignement d'Ararat entre le Grand et Petit Ararat, localisation sur la figure 10. A : sur une image satellite, B : interprétation, 1 : volcans, 2 : failles supposées, 3 : volcans supposés.

from the same geological formation corresponding to different stress orientations [64].

Only at a few sites is nearly uniform compression orientation observed. To the east of the Black Sea (1 on figure 10) the orientation of the principal stress is NW-SE. More to the east (2 on figure 10) the orientation is principally NNE-SSW. Otherwise the stress orientations are dominantly N-S, NW-SE and NE-SW as we can see in the rose diagram for all data collected in geological formations from Proterozoic to Quaternary (Fig. 13). To study the paleo-stress data as a function of the geological formation ages we took into account the stations with confident geological ages. Few measurements (7 stations) have been realized in Paleozoic formations (Devonian to Permian), 24 stations are measured in Mesozoic formations, 18 in Paleogene and about 16 in Neogene to Quaternary formations.

The structures and the finite strain fields are the result of several stress phases reflecting the tectonics evolution of the region during collisional events. Neogene to Quaternary formations have only been affected by the last stress phases related to the indentation of the Arabian plate. Consequently, to analyse the stress evolution with time during the last collision events we have distributed the calculated compression (σ_1) axis according to the geological formation age. In the given age formation the latest stress can and the earliest stress cannot be observed.

On figure 13, we note that compression orientations are significantly different in the various geological formations; though being N-S on average. In all cases the above-mentioned three stress orientations (N-S, NE-SW and NW-SE) are present. In the Neogene to Quaternary formations the dominant directions are NNE-SSW and NE-SW. It is NE-SW and NW-SE for the Paleogene formations. It is N-S and NW-SE for the Jurassic to Cretaceous formations and it is NE-SW with general N-S orientations for Devonian to Permian formations.

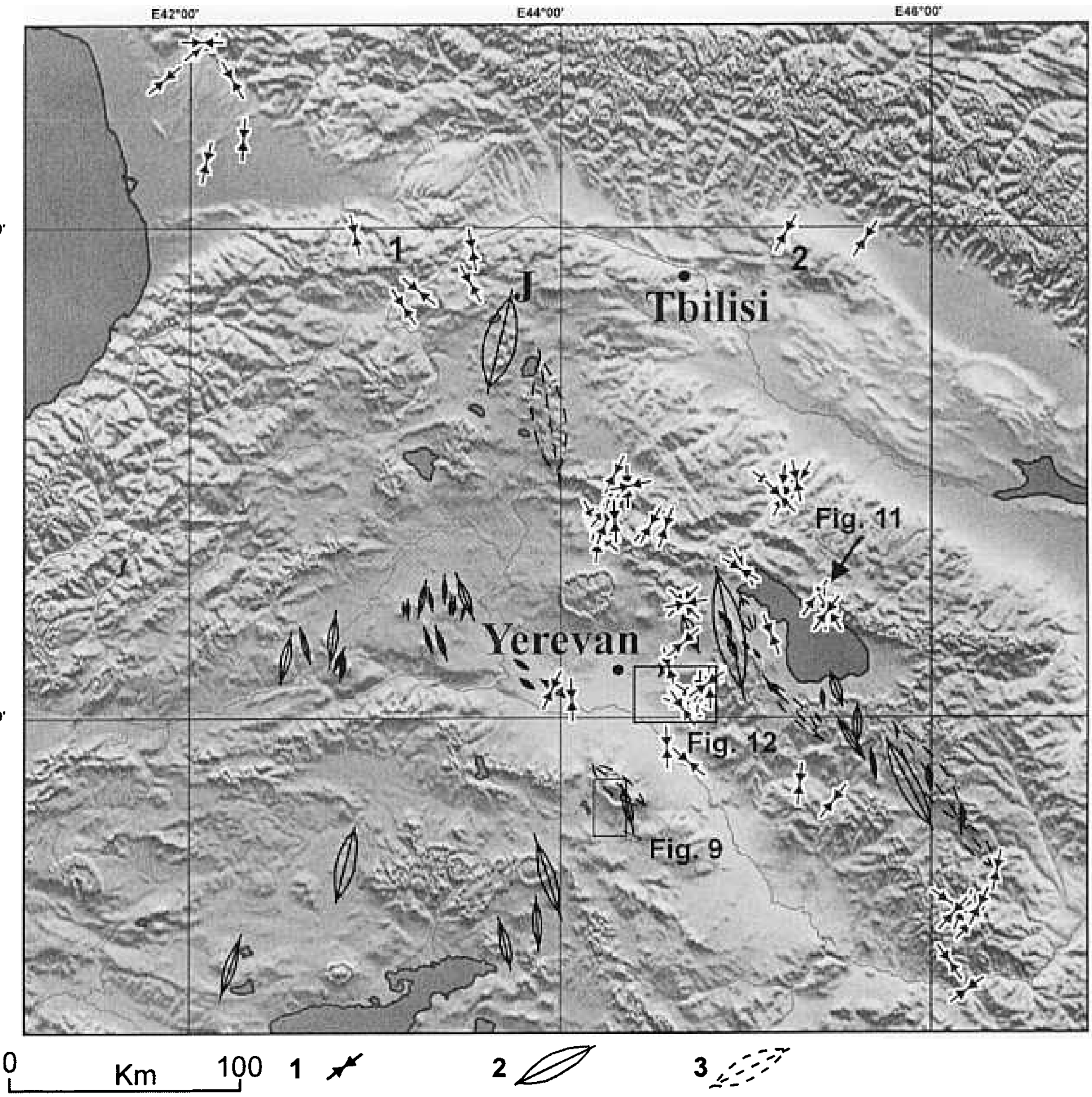

Fig. 10 Horizontal component of the principal compression stress orientations from microtectonic data and volcanic clusters (microtectonic data from Philip *et al.* (1989) for southern Georgia; and clusters data of Adyaman *et al.* (1998) for Eastern Turkey are also used). 1: compression axis, 2: volcanic clusters recognized with confidence, 3: supposed volcanic clusters.

Composante horizontale des orientations du principal champ de contrainte à partir des données microtectoniques et des alignements volcaniques (données microtectoniques de Philip *et al.* (1989) pour la Géorgie du sud ; et alignements volcanique de Adÿaman *et al.* (1998) pour l'Est de la Turquie. 1 : axe de compression, 2 : alignements volcaniques bien reconnus, 3 : alignements volcaniques supposés.

6. Discussion and conclusion

The stress indicators including Neogene to Quaternary volcanic cluster orientation, fault kinematics data, focal mechanisms P axis and GPS data [18, 24, 30, 31, 32, 33, 44, 60, 61, 62 and 63] show the scale and temporal changes in stress and strain fields since the Arabian-Eurasian collision.

To interpret the stress evolution from the Neogene to Quaternary we must consider block rotation effects as a consequence of the continental collision. The paleomagnetic data [e.g. 15, 17, 25, 66 and 67] show that the sense of rotation is not the same in different blocks of the area. The main blocks have been affected by rotation during late stages of the continental collision (Fig. 3). Rotations are clockwise to the East and anti clockwise to the West from Arabian wedge tip [e.g. 15 and 25]. A similar situation is observed in the northern areas of the Armenian structural wedge (Ar on Fig. 2) formed by indentation of the derived from Gondwana

Fig. 11 Example of fault kinematics change on the same fault plane in the Upper Cretaceous series, location on figure 10. A: - Fault plane in the Upper Cretaceous pelagic limestones, B:- Striations S1 and S2 on the slikenside correspond to two kinematics events.

Un exemple de deux mouvements sur un plan de faille dans les calcaires pélagiques du Crétacé supérieur (localisation sur la figure 10). A : Plan de faille, B : Stries S1 et S2 sur le plan de rupture matérialisant deux mouvements distincts le long de la faille.

rigid blocks [66 and 67]. Most of the used fault kinematics stress indicators of the Lesser Caucasus are situated in the South Armenian block of Gondwana origin.

According to fault kinematics data, the NW-SE compressive stress orientation is quite significant in the Jurassic to Palaeogene formations but absent in the Neogene to Quaternary ones. Previous fault kinematics results from the Eurasian margin (Great Caucasus) show evidence for a NW-SE trend of compression in the Mesozoic formations mainly due to an Eocene transpressional stress field [68]. On the other hand our fault kinematics data are derived from the Lesser Caucasus area and concern the Gondwanian block and the Mesozoic Eurasian margin series in the North Lesser Caucasus which collided together during Paleogene times (Fig. 3). Consequently, we assume that this NW-SE compression direction characterizes the Paleogene stress field due to the collision (Fig. 13). The results are consistent with the geological data indicating NW-SE Arabian-Eurasian convergence since the beginning of the Lower Oligocene period [17].

Fault kinematics data from the Neogene to Quaternary series are consistent with a change in the convergence direction during the Middle Miocene, which became submeridian to NNE-SSW in the East [15]. The NE-SW compression orientation in Paleogene formations can be due to farther Neogene-Quaternary stress field (Fig. 13).

The volcanic cluster data clearly indicate three compressional orientations in the whole area. In contrast to the fault kinematics data the volcanic cluster orientation data show space distribution regularity. They form a wedge with tip to the North like active fault. This is evidence for the genetic relationship between active faults and volcanism. One part of Neogene to Quaternary volcanism is rooted on normal fault systems or on strike-slip fault pull-apart structures [41, 44, 46 and 51].

If we take into account the scarce microtectonic stations for fault kinematics analyses obtained in the Neogenes series (14 stations from 16 measured in Quaternary rocks) showing N-S and NE-SW compression orientation and volcanic clusters suggesting NNW-SSE shortening one (Fig. 7), we can suppose that Quaternary structures controlling volcanism in the Lesser Caucasus area are inherited from former NW-SE Paleogene-Neogene faults. These inherited structures also influence the farther stress field as shown from GPS extension data with an azimuth of N 55° in the same area [60].

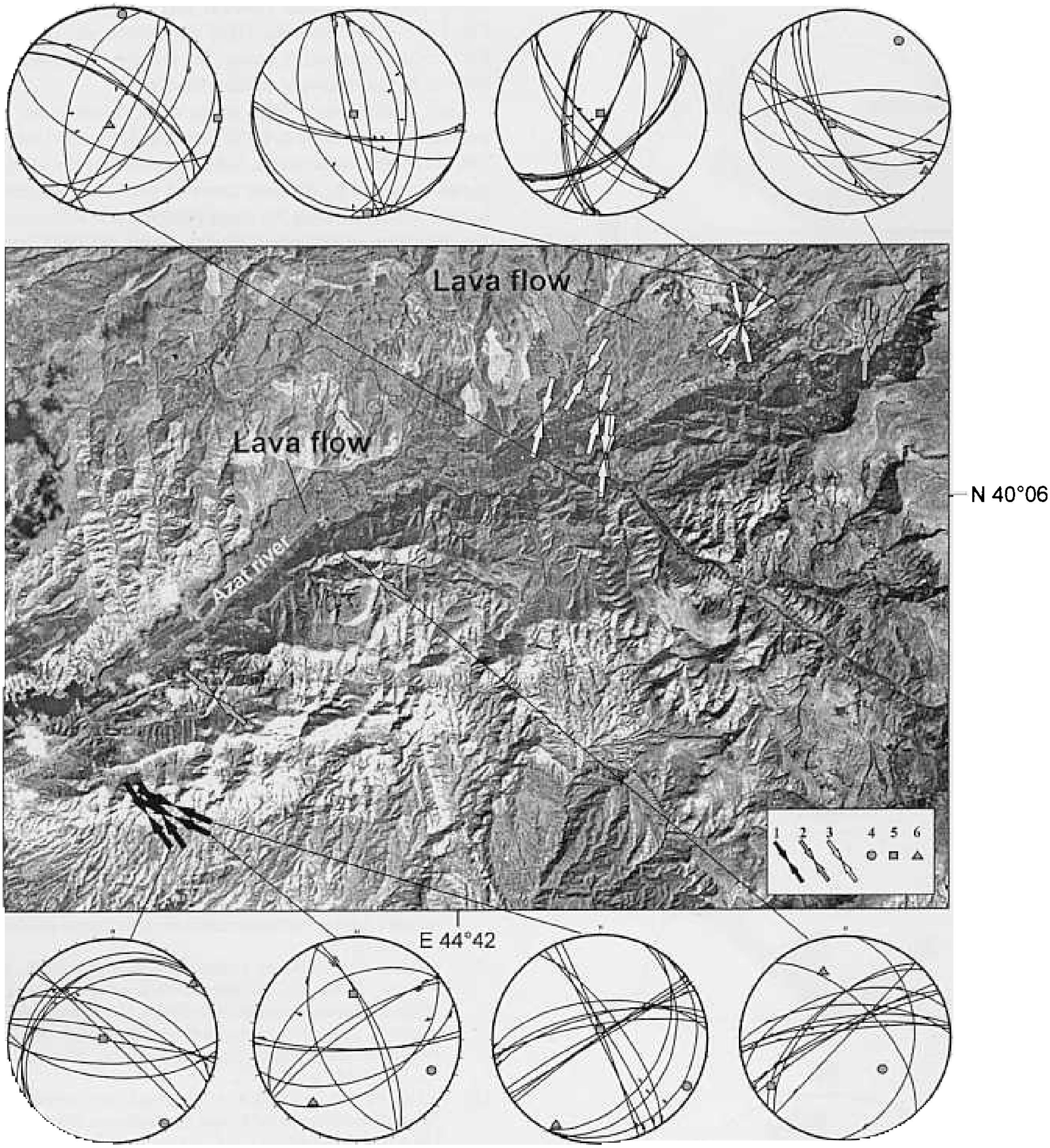

Fig. 12 Fault kinematics data in the Azat river area (location is shown on figure 10). Data obtained from 1: Cretaceous formations, 2: Paleogene formations, 3: Quaternary formations; paleo-stress axes: 4: σ_1, 5: σ_2, 6: σ_3.

Données microtectoniques de la région de la rivière Azat (localisation sur la figure 10). Les données ont été obtenues sur 1 : les formations crétacées, 2 : les formations paléogènes, 3 : les formations quaternaires; paléo-axes des contraintes: 4 : σ_1, 5 : σ_2, 6 : σ_3.

While an overall N-S shortening orientation can be derived from fault kinematics/volcanic cluster data, more secondary NE-SW and NW-SE compression is also noted. We interpret these two orientations as being the result of two distinct tectonic phases when they were dominant.

GPS data suggest NNE shortening in the Trans-Caucasian region (corresponding to main NW-SE trend of the mountain range). At the same time, on the large scale they show an extension strike of about N 60° E as indicated by Neogene-Quaternary volcanic clusters and fault kinematics data in the

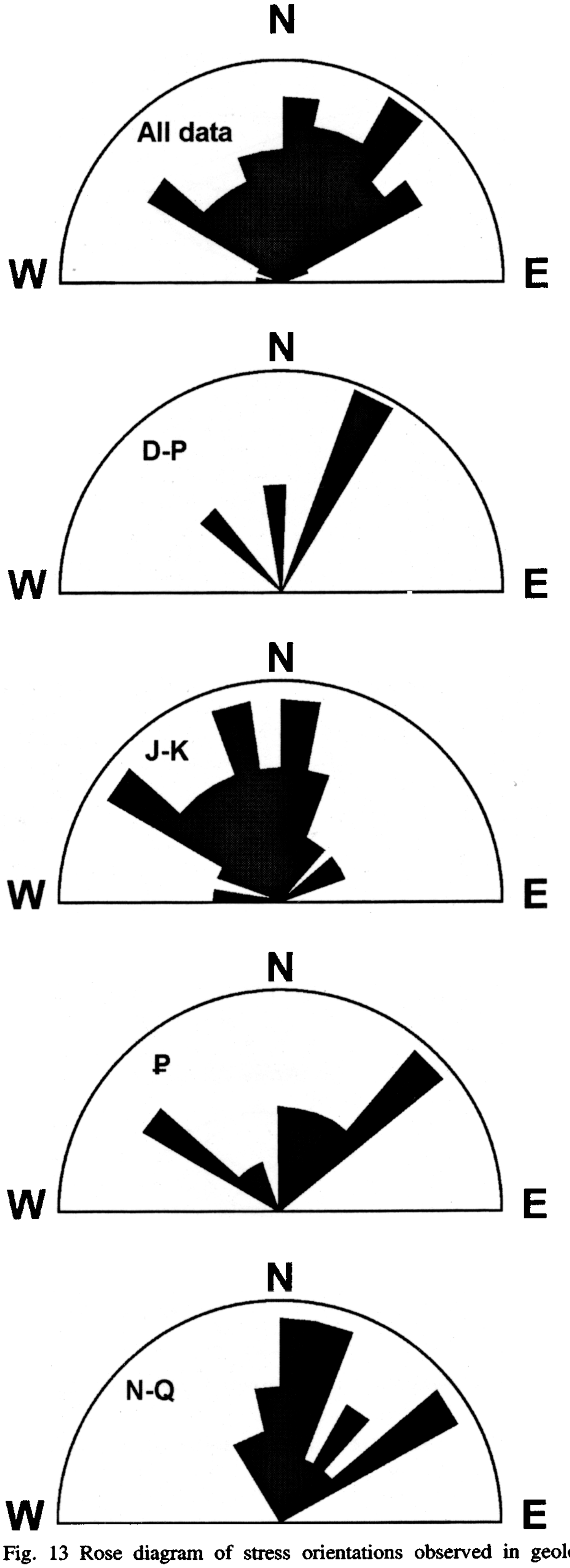

Fig. 13 Rose diagram of stress orientations observed in geological formations of different ages (D-P: Devonian to Permian, J-K: Jurassic and Cretaceous, P: Paleogene, N-Q: Neogene and Quaternary).

Diagrammes en rosace de l'orientation de la composante horizontale de la contrainte principale σ_1 observée dans des roches d'âge différent. (D-P : Dévonien à Permien, J-K : Jurassique à Crétacé, P : Paléogène, N-Q : Néogène à Quaternaire).

South Armenian block (central part of the studied area; Fig. 1). It coherent with GPS data obtained in Iran by French-Iranian research group [31] and can be explained by the role of the relatively smaller blocks.

Our studies show that stress axes orientations have evolved with time due to geodynamic conditions in the area. These changes in the stress field are related to the changing regime imposed by Arabian-Eurasian plate convergence. At a smaller tectonic scale the stress orientation is influenced by the dynamics of secondary blocks. Some of block borders correspond to lithospheric border plates such as the South Armenia block (Fig. 1) of Gondwana origin. The other borders correspond to crustal faults probably inherited from the Meso-Cenozoic tectonic evolution and result from a combination of obduction and collisions (Gondwanian blocks and Arabia).

Acknowledgements

This work was supported by the NATO post-doctoral award. The authors would like to thank Professeur J-F Stéphan (UMR Géosciences Azur, Université de Nice Sophia-Antipolis), Dr R. Jrbashian (Institut of Geological Sciences, Armenia) for their valuable support. This paper benefited greatly from the comments of J. Piper and one anonymous reviewer. Publication n° 803 of UMR Géosciences Azur, CNRS.

References

[1] Dercourt J., Zonenshain L.P., Ricou L.-E., Kazmin V.G., Le Pichon X., Knipper A.L., Grandjacquet C., Sbortshikov I.M., Geyssant J., Lepvrier C., Pechersky D.H., Boulin J., Sibuet J.-C., Savostin L.A., Sorokhtin O., Westphal M., Bazhenov M.L., Lauer J.P., Biju-Duval B., Geological evolution of the Tethys belt from the Atlas to the Pamirs scince the Lias, Tectonophysics 123 (1986) 241-315.

[2] Nikishin, A.M., Cloetingh, S., Brunet, M.-F., Stephenson, R., Bolotov, S.N., Ershov A.V., Scythian Platform and Black Sea region: Mesozoic–Cenozoic tectonic and dynamics, in: Crasquin-Soleau, S., Barrier, E. (Eds.), Peri-Tethys Memoir 3: Stratigraphy and Evolution of Peri-Tethyan Platforms, Mém. Mus. natn. Hist. nat., Paris, vol. 177, (1998), pp. 163–176.

[3] Robertson, A.H.F., Overview of the genesis and emplacement of Mesozoic ophiolites in the Eastern Mediterranean Tethyan region , Lithos 65 (2002) 1-67.

[4] Golonka, J., Plate tectonic evolution of the southern margin of Eurasia in the Mesozoic and Cenozoic, Tectonophysics 381 (2004) 235-27.

[5] Jackson, J.A., McKenzie, D.P., Active tectonics of the Alpine—Himalayan Belt between western Turkey and Pakistan, Geophys. J. R. Astron. Soc. 77 (1984) 185-264.

[6] Philip H., Avagyan A., Karakhanian A., Ritz J-F., Rebai S., Slip Rates and Recurrence Intervals of Strong Earthquakes along the Pambak-Sevan-Sunik Fault (Armenia), Tectonophysics 343, 3-4 (2001) 205-232.

[7] Rebaï S., Philip H., Dorbath L., Borissoff B., Haessler H., Cisternas A., Active tectonics in the Lesser Caucasus: Coexistence of compressive and extensional structures. Tectonics, October, vol. 12, N°5 (1993) 1089-1114.

[8] Trifonov V.G., Sobolva O.V., Trifonov R.V., Vostrikov G.A., Recent geodynamic of Alp-Himalayan collision belt (Ed), Leonov U.G., Moskva, GEOS (2002) 224.

[9] McKenzie, D.P., Active tectonics of the Mediterranean region. Geophys. J. R. Astron. Soc. 30 (1972) 109-185.

[10] Sengör, A.M.C., Kidd, W.S.F., Post-collisional tectonics of the Turkish–Iranian plateau and a comparison with Tibet. Tectonophysics 55 (1979) 361-376.

[11] Dewey, J.F., Hempton, M.R., Kidd, W.S.F., Saroglu, F., Sengör, A.M.C., Shortening of continental lithosphere: the neotectonics of Eastern ANATOLIA—a young collision zone. Spec. Publ.-Geol. Soc. London 19 (1986) 3-36.

[12] Taymaz, T., Jackson, J., McKenzie, D., Active tectonics of the north and central Aegean sea. Geophys. J. Int. 106 (1991) 433-490.

[13] Karakhanian A.S., Trifonov V.G., Philip H., Avagyan A., Hessami K., Jamali F., Bayraktutan S.M., Bagdassarian H., Arakelian S., Davtian V., Active Faulting and Natural Hazards in Armenia, Eastern Turkey and North-western Iran. Tectonophysics 380 (2004) 189-219.

[14] Biju-Duval, B.J., Dercourt J., Le Pichon, X., From the Tethys Ocean to the Mediterranean seas: a plate tectonic model of the evolution of western Alpine System. In: Biju-Duval, B., Montadert, L. (Eds.), Structural History of the Mediterranean Basins. Ed. Technip, Paris (1977) 143-164.

[15] Zonenshain L.P., Dercourt J., Cazmin V.G., Ricou L.E., Knipper A.L., Le Pichon X., Sborshikov I.M., Grandjacquet C., Pecherski D.M., Geissant J., Lepvrier C., Savostin L.A., Sorokhtin O.G., Bulen G., Sibuet J-C., Bagenov M.L., Bestfal M.B., Lauer G.P., Bigu-Duval B., Tethys evolution. In: Geological history of the Tethys ocean. Academy of sciences of the USSR, P.P.Shirshov Institute of Oceanology, Moscow, 1987, pp. 104-115.

[16] Livermore, R.A., Smith, R.G., Relative motions of Africa and Europe in vicinity of Turkey In Geology of the Taurus Belt. In: Tekeli, O., Goncuoglu, M.C. (Eds.), Proceedings of an International Symposium on the Geology of the Taurus Belt. Maden Tetkik ve Arama, Ankara (1984) 1-10.

[17] Savostin L.A., Sibuet J.-C., Zonenshain L.P. *et al.*, Kinematic evolution of the Tethys belt from the Atlantic Ocean to the Pamirs since the Triassic/Tectonophysics. Vol.123, N 1/4 (1986) 1-35.

[18] Philip H., Cisternas A., Gvishiani A., Gorshkov A., The Caucasus: an actual example of the initial stage of continental collision. Tectonophysics 161 (1989) 1-21.

[19] Ricou L-E., Tethys reconstucted : plates, continental fragments and their Boundaries since 260 Ma from Central America to South-eastern Asia. Geodynamica Acta (Paris), 7, 4 (1994) 169-218.

[20] Le Pichon, X., Gaulier, J.M., The rotation of Arabia and the Levant fault system. Tectonophysics 153 (1988) 271-294.

[21] Dewey, J.F., Pitman, W.C. III, Ryan, W.B.F., Bonnin, J., Plate tectonics and the evolution of the Alpine System. Geol. Soc. Am. Bull. 84 (1973) 137-3180.

[22] Yilmaz, Y., New evidence and model of the evolution of the southeast Anatolian orogen. Geol. Soc. Am. Bull. 105 (1993) 252-271.

[23] Platzman, E.S., Platt, J.P., Tapirdamaz, C., Sanver, M., Rundle, C.C., Why are there no clockwise rotations along the North Anatolian Fault Zone, Turkey. J. Geol. Res. 99 (1994) 21705-21715.

[24] Reilinger, R.E., McClusky, S.C., Oral, M.B., King, R.W., Toksoz, M.N., Barka, A.A., Kinik, I., Lenk, O., Sanli, I., Global Positioning System measurements of present day crustal movements in the Arabia–Africa–Eurasia plate collision zone. J. Geophys. Res. 102 (1997) 9983-9999.

[25] Gürsoy H., Piper J.D.A., Tatar O., Neotectonic deformation in the western sector of tectonic escape in Anatolia: palaeomagnetic study of the Afyon region, central Turkey. Tectonophysics 374 (2003) 57-79.

[26] Joffe, S., Garfunkel, Z., Plate kinematics of the Circum Red Sea, a reevaluation. Tectonophysics 141 (1987) 5-22.

[27] DeMets, C., Gordon R. G., Argus D. F., and Stein S., Effect of recent revisions to the geomagnetic time scale on estimates of current plate motion. Geophys. Res. Lett., 21 (1994) 2191-2194.

[28] DeMets, C., Gordon R.G., Argus D.F., and Stein S., Current plate motions. Geophys. J. Int., 101 (1990) 425-478.

[29] Milanovski E.E., Neotectonics of the Caucasus, Nedra, Moscow, (in Russian) 1968, 484 p.

[30] McClusky S., Balassanian S., Barka A., Demir C., Ergintav S., Georgiev I., Gurkan O., Hamburger M., Hurst K., Kahle H., Kastens K., Kekelidze G., King R., Kotzev V., Lenk O., Mahmoud S., Mishin A., Nadariya M., Ouzounis A., Paradissis D., Peter Y., Prilepin M., Reilinger R., Sanli I., Seeger H., Tealeb A., Toksöz M.N., Veis G., Global Positioning System constraints on plate kinematics and dynamics in the eastern Mediterranean and Caucasus. Journal of Geophysical Research, 105, B3 (2000) 5695-5719.

[31] Vernant Ph., Nilforoushan F., Hatzfeld D., Abbassi M.R., Vigny C., Masson F., Nankali H., Martinod J., Ashtiani A., Bayer R., Tavakoli F., Chery J., Present-day crustal deformation and plate kinematics in the Middle East constrained by GPS measurements in Iran and northern Oman, Geophys. J. Int. 157 (2004) 381-398.

[32] Tovmassian A.K., Arakelian A.R., Harutunian R.S., Results of stress field investigation in the territory of Armenia and adjacent regions. In. Giardini D., Balassanian S. (Eds.), Historical and Prehistorical Earthquakes in the Caucasus, Kluwer Academic Publishers, Printed in Netherlands, (1997), pp. 471-483.

[33] Hessami K., Jamali F., Tabassi H., Map: Major active faults of Iran. International Institute of Earthquake Engineering and Seismology, Tehran (2003).

[34] Argus, D.F., Gordon R.G., No-net-rotation model of current plate velocities incorporating plate motion model NUVEL-1, Geophys. Res. Lett., 18 (1991) 2039-2042.

[35] Drewes, H., Combination of VLBI, SLR, and GPS determined station velocities for actual plate kinematic and crustal deformation models, Geodynamics, M. Feissel (Eds.), IAG Symposia, Springer (1998).

[36] Drewes, H., D. Angermann, The Actual Plate Kinematic and Crustal Deformation Model 2000 (APKIM2000) as a Geodetic Reference System, AIG 2001 Scientific Assembly, Budapest, 2-8 Sept (2001).

[37] Kreemer, C., Global Strain Rate Map Project; Corné Kreemer kindly provided NNR poles of rotation for version 1.2, May (2004).

[38] Sella, G.F., Dixon T.H., and Mao A., REVEL: A model for recent plate velocities from space geodesy, J. Geophys. Res., 107, B4, 10.1029/2000JB000033 (2002).

[39] Yunga S.L., Seismotectonic deformation of the Northern Eurasia Fold Belts in the Neotectonic Phase. Izvestia, Physics of the Solid Earth, Vol. 32, N°12 (1996) 37-58.

[40] Shirinian K.G., Report: Catalogue of Upper Pliocene—Quaternary volcanoes of Armenian SSR. Institute of Geological Sciences, NAS of RA, Erevan (1978).

[41] Innocenti F., Mazzuoli R., Pasquare G., Serri C., Villari L., Geology of the volcanic area north of Lake Van (Turkey). Geol. Rundsch. 69 (1980) 292-322.

[42] Karapetian, K.I., Areal volcanism in the Armenian SSR. Final Report of the Institute of Geological Sciences of the Armenian SSR Academy of Sciences, Yerevan, (1985) 319 p.

[43] Ferraud, J., Les volcans actifs de Turquie: Guide géologique et itinéraires d'excursions, Mémoire de l'Association Volcanologique Européenne, ISSN 0982-9601, 2 (1994) 140 p.

[44] Adiyaman O., Chorowicz J., Kose O., Relationships between volcanic patterns and neotectonics in Eastern Anatolia from analysis of satellite images and DEM. Journal of Volcanology and Geothermal Research 85, (1998) 17-32.

[45] Karapetian S.G., Jrbashian R.T., Mnatsakanian A. Kh., Late collision rhyolitic volcanism in the north-eastern part of the Armenian Highland, Journal of Volcanology and Gothermal Reasearch, 112 (2001) 189-220.

[46] Karakhanian A., Djrbashian R., Trifonov V., Philip H., Arakelian S., Avagian A., Holocene-historical volcanism and active faults as natural risk factors for Armenia and adjacent countries, Journal of Volcanology and Geothermal Research, 113, 1-2, March (2002) 319-344.

[47] Karakhanian A., Jrbashyan R., Trifonov V., Philip H., Arakelian S., Avagyan A., Baghdassaryan H., Davtian V., Ghoukassyan Yu., Volcanic Hazards in the Region of the Armenian Nuclear Power Plant. Journal of Volcanology and Geothermal Research. 126 (2003) 31-62.

[48] Melkonyan R.L., Petrology, mineralogy and geochemistry intrusive formations of Alaverdy ore area. In. Meliksetyan B.M., Melkonyan R.L., Petrology, mineralogy and geochemistry intrusive formations of some ore areas of Armenian SSR. Izdatatelstvo Academy of Sciences of Arm. SSR, (in Russian), (1976) 137-279.

[49] Adamia S. A, Chkhotua T., Kekelia M., Lordkipanidze M., and Shavishvili I., Tectonics of the Caucasus and adjoining regions: Implications for the evolution of the Tethys ocean. J. Struct. Geol., 4 (1981) 437-447.

[50] Innocenti, F., Manetti, P., Mazzuoli, R., Pasquare, G., Villari, L., Anatolia and North-Western Iran. In: Thorpe, R.S. (Ed.), Andesites: Orogenic Andesites and Related Rocks. The Open Univ., Dep. Earth Sci., Milton Keynes, UK (1982) 327-349.

[51] Yilmaz, V., Güner, Y., Saroglu, F., Geology of the Quaternary volcanic centers of the East Anatolia. J. Volcanol. Geotherm. Res. 85 (1998) 173-210.

[52] Avagyan, A., Estimation of slip rates and recurrence intervals of strong earthquakes on the fault system of Pambak-Sevan-Sunik (Armenia): segmentation and relation with volcanic ctivity. PhD Thesis, Montpellier II University, France, (2001) 238 p.

[53] Avagyan A., Karakhanian A., Philip H., Une éruption volcanique gravée dans le roc. Pour la science. N°305, mars (2003) 13-14.

[54] Nakamura, K., Arrangement of parasitic cones as a possible key to regional stress field. Volcanol. Soc. Jpn. Bull. 14 (1969) 8-20.

[55] Jackson, E.D., Shaw, H.R. Stress fields in central portions of the Pacific plate: delineated in time by linear volcanic chains. J. Geophys. Res. 80 (1975) 1861-1874.

[56] Opheim, J.A., Gudmundsson, A., Formation and geometry of fractures, and related volcanism of the Krafla fissure swarm, Northeast Iceland. Geol. Soc. Am. Bull. 101 (1989) 1608-1622.

[57] Chorowicz, J., Bardintzeff, J.M., Rasamimanana, G., Chotin, P., Thouin, C., Rudant, J.P., An approach using SAR ERS images to relate extension fractures to volcanic vents: examples from Iceland and Madagascar. Tectonophysics 271 (1997) 263-283.

[58] Koyaguchi, T., Takada, A., An experimental study on the formation of composite intrusions from zoned magma chambers. J. Volcanol. Geotherm. Res. 59 (1994) 261-267.

[59] Bellier, O., Sebrier, M., Relationship between tectonics and volcanism along the great Sumatran fault zone deduced by SPOT image analysis. Tectonophysics 233 (1994) 215-231.

[60] Doerflinger, E., Karakhanian, A., Philip, H., Avagyan, A., Masson, F., Aslanian, R., Bayer, R., Jrbashyan, R., Vernant, P, Davtyan, V., Champollion, C., Hamard, E. Fault activity constrained by GPS data in Armenia. (in preparation) (2005).

[61] Pistre S., Arthaud F. & Simonian G., Compression et distension simultanées dans un basin sédimentaire en zone sismique. Cas du basin de Spitak (Armenie).—C.R. Acad. Sci. Paris, 320 (1995) 1011-1016.

[62] Avagyan A., Analysis of microtectonics data for the epicentral zone of the 1988 Spitak earthquake and central part of the territory of the Republic of Armenia. Izvestia NAS of RA, "Nauki o Zemlie" 1-2 (1997) 94-98.

[63] Arthaud F., Leonardi V., Avanessian A., Avagyan A., Grillot J-C., Effets des déformations tectoniques sur le comportement hydraulique d'un aquifère artésien dans une région sismique (Arménie), Bull. Soc. Géol. France, 4 (1998) 579-588.

[64] Tayan R.N., Tectonic stresses in the Permian limestones of the Gueghi river middle course (western Zanguezoor), Izvestia NAS of RA, XXXIII, 4, (1980) 49-55.

[65] Etchecopar A., Vasseur G., and Daignieres M., An inverse problem in microtectonics for determination of stress tensors from fault striation analysis. J. Struct. Geol., 3 (1981) 51-65.

[66] Adamia S.A., Asanize B.Z., Gambashize R.A., Paleo-magnetism upper Cretaceous rock of the southern Georgia and geological interpretation. Izv. ASc. SSSR. Serie Geol. N 5 (1979) 46-57.

[67] Bazhenov M.L., Burtman V.S., Levashova N.L., Lower and Middle Jurassic paleomagneric results from the south Lesser Caucasus and the evolution of the Mesozoic Tethys ocean. Earth and Planetary Science Letters, 141 (1996) 79-89.

[68] Sebrier M., Polino R., Galkine V., Yunga S., Caucasus Stress Evolution from Mesozoic to Present. EUG 9, Strasbourg, 23-27 March 1997, Abstract supplement N°1 to Terra Nova, 9 (1997) 337.